AIP Journal of Applied Physics

Analysis of heterostructures for electroluminescent refrigeration and light emitting without heat generation

Shun-Tung Yen and Kuan-Chen Lee

Citation: Journal of Applied Physics **107**, 054513 (2010); doi: 10.1063/1.3326944
View online: http://dx.doi.org/10.1063/1.3326944
View Table of Contents: http://scitation.aip.org/content/aip/journal/jap/107/5?ver=pdfcov
Published by the AIP Publishing

Articles you may be interested in

Scanning tunneling microscope-based local electroluminescence spectroscopy of p-AlGaAs/i-GaAs/n-AlGaAs double heterostructure
J. Vac. Sci. Technol. B **30**, 021802 (2012); 10.1116/1.3684985

Photon recycling effect on electroluminescent refrigeration
J. Appl. Phys. **111**, 014511 (2012); 10.1063/1.3676249

Self-heating and athermal effects on the electroluminescence spectral modulation of an AlGaInP light-emitting diode
J. Appl. Phys. **110**, 073103 (2011); 10.1063/1.3643005

Analysis of optothermionic refrigeration based on semiconductor heterojunction
J. Appl. Phys. **99**, 074504 (2006); 10.1063/1.2188249

Room-temperature semiconductor heterostructure refrigeration
Appl. Phys. Lett. **87**, 022103 (2005); 10.1063/1.1992651

Re-register for Table of Content Alerts

Create a profile.

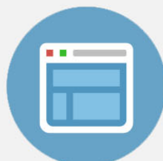

Sign up today!

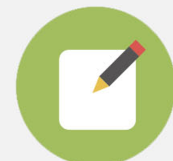

[This article is copyrighted as indicated in the article. Reuse of AIP content is subject to the terms at: http://scitation.aip.org/termsconditions. Downloaded to] IP: 140.113.38.11 On: Wed, 30 Apr 2014 11:57:17

Analysis of heterostructures for electroluminescent refrigeration and light emitting without heat generation

Shun-Tung Yen[a] and Kuan-Chen Lee
Department of Electronics Engineering and Institute of Electronics, National Chiao Tung University, 1001 Ta-Hsueh Road, Hsinchu 30050, Taiwan

(Received 18 September 2009; accepted 20 January 2010; published online 10 March 2010)

We perform a self-consistent calculation to investigate the feasibility of electroluminescent refrigeration and light emitting without heat generation in AlGaAs/GaAs heterostructures, taking into account the effects of various recombination processes. The effect of radiation extraction on the cooling capacity and efficiency is also considered. Carrier blocking layers are used to almost eliminate current leakage and improve the injection efficiency to nearly 100%. An analysis is presented of the cooling power density, the cooling efficiency, and the radiative power density as functions of the applied voltage. We also explore the dependences of the cooling related quantities on the thickness and the doping of the active region. A GaAs active layer of thickness 5 μm at 300 K can give a limiting cooling power density of 97 W/cm^2. We show that a net cooling power (>several W/cm^2) and a high-power light emitting (>100 W/cm^2) without heating are feasible. They require an overall efficiency of more than 90%, which is easily achieved if the photon recycling efficiency is high. © *2010 American Institute of Physics*. [doi:10.1063/1.3326944]

I. INTRODUCTION

The area of solid-state refrigeration by luminescence upconversion has progressed rapidly[1] since the first successful observation of net cooling in ytterbium-doped glass.[2] The photoluminescent (PL) coolers have advantages of compactness, high reliability, and the absence of vibrations and cryogen, which the conventional thermoelectric (TE) coolers have. In addition, it has been realized that the PL coolers can outperform the TE cooler at cryogenic temperature.[3,4] Much attention has been spent on examining the PL cooling in semiconductors both theoretically[5–7] and experimentally.[8–11] The semiconductor PL coolers are expected to have the potential of higher cooling power and lower temperature operations compared to the rare-earth doped glass coolers, and the opportunity to be integrated epitaxially with other electronic and photonic semiconductor devices. The PL cooling requires an external quantum efficiency (EQE) of nearly 100%, and hence can occur only in a device that is made of high-purity materials and has a specially designed geometry. Such a harsh requirement has rendered the luminescent cooling in semiconductors unattainable.[8–11]

The requirement for cooling action in semiconductors through photon emission can be alleviated by using electric injection instead of optical pumping. It has been known for a long time that heat can be removed from the lattice in a forward-biased diode when the electric work on each injected electron qV is lower than the average emitted photon energy $\langle \hbar\omega \rangle$, where q is the elementary charge and V is the applied voltage.[12,13] The electroluminescent (EL) cooling can be achieved if the EQE is higher than $qV/\langle \hbar\omega \rangle$, while the PL cooling requires an EQE of at least $E_g/\langle \hbar\omega \rangle$, where E_g is the band gap of the material. Since $\langle \hbar\omega \rangle \approx E_g + k_BT$, where k_B is the Boltzmann constant and T is the temperature, the minimum EQE required for PL cooling must be close to unity if $k_BT \ll E_g$, but that for EL cooling is adjustable and can be significantly lower than unity depending on V. The *pn* junction diode can work as a radiant heat engine which exchanges radiation with the environment.[14] Berdahl[14] suggested a narrow-gap semiconductor diode of $E_g \sim$ several k_BT for cooling its radiant environment in the reverse-biased mode, as well as for cooling the diode itself by electroluminescence in the forward-biased mode. His analysis demonstrates that the effect of the parasitic loss in the reverse-biased cooling mode is much less dramatic than in the forward-biased mode, at the price of the cooling capacity. Mal'shukov and Chao[15] proposed a semiconductor heterostructure for EL cooling with a central active region embedded between *p*-cladding and *n*-cladding layers. They investigated quantitatively the effect of the Auger nonradiative recombination on the heat pumping in the heterostructure. In the ideal case that the generated photons can totally escape out of the structure, a cooling rate of tens of W/cm^2 can be achieved.[15] Further studies on the EL refrigeration have focused on optimization of the active region for a high cooling rate.[16–18] It has been pointed out that a high three-dimensional density of states is preferred for a high cooling rate because it enhances the radiative recombination in the active region.[16] However, the abovementioned studies about EL cooling in the heterostructure do not consider seriously the effects of the carrier injection efficiency and the photon extraction on the cooling capacity. These effects are critical to attaining the net cooling in a forward-biased diode.

Very recently, Heikkilä *et al.*[19] have analyzed a similar heterostructure using a simple model considering various loss mechanisms. Different from the previous work, their study focused on optimizing the structural and material parameters to find out the ultimate limit of efficiency for light-

[a]Electronic mail: styen@cc.nctu.edu.tw.

 © 2010 American Institute of Physics

[This article is copyrighted as indicated in the article. Reuse of AIP content is subject to the terms at: http://scitation.aip.org/termsconditions. Downloaded to] IP: 140.113.38.11 On: Wed, 30 Apr 2014 11:57:17

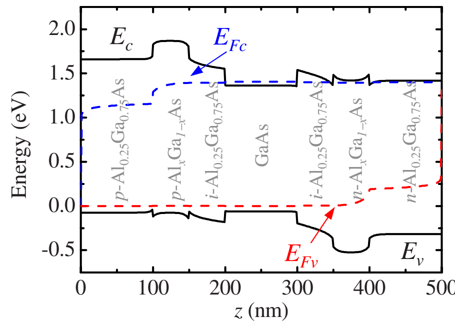

FIG. 1. (Color online) The energy band profiles, E_c and E_v, and the quasi-Fermi level profiles, E_{Fc} and E_{Fv}, along the growth direction z of the conduction and the valence bands, respectively, for the heterostructure under consideration. The profiles are a result of our self-consistent calculation at a forward bias of 1.4 V.

emitting applications but not for refrigeration applications. There is a compromise between the cooling efficiency and the cooling power (or the radiation power). The trade-off depends on the purpose for which the device is designed.

In this paper, we formulate and then perform a self-consistent calculation[20] to investigate the feasibility of EL refrigeration in a heterostructure, taking into account the effects of various nonradiative recombination losses. The effect of radiation extraction efficiency on the EL cooling is also considered. Emphasis will be not only on the cooling capacity but also on the light emitting without heat generation. Carrier blocking layers are introduced to effectively eliminate current leakage and improve the injection efficiency. We then analyze the cooling power density, the cooling efficiency, and the radiative power density as functions of the applied voltage. We also explore the effects of the thickness and the doping of the active region. We find that a cooling power of several W/cm^2 and high-power light emitting (more than 100 W/cm^2) without heat generation require an overall efficiency of more than 90%. The high overall efficiency is feasible if the photon recycling efficiency is high.

The paper is organized as follows. In Sec. II, we will describe the theoretical approaches including a self-consistent model and formulation for quantities of interest. Calculated results together with analysis and discussion will be presented in Sec. III. Finally, we draw a conclusion in Sec. IV.

II. THEORETICAL APPROACHES

A. Self-consistent model

We consider a heterojunction structure, as illustrated in Fig. 1, composed of seven layers; they are, in order, a 100 nm p-$Al_{0.25}Ga_{0.75}As$ cladding layer (acceptor concentration $N_a = 10^{18}$ cm^{-3}), a 50 nm p-$Al_xGa_{1-x}As$ electron blocking layer ($x \geqslant 0.25$, $N_a = 10^{18}$ cm^{-3}), a 50 nm undoped $Al_{0.25}Ga_{0.75}As$ spacer layer, a GaAs active layer, a 50 nm undoped $Al_{0.25}Ga_{0.75}As$ spacer layer, a 50 nm n-$Al_xGa_{1-x}As$ hole blocking layer (donor concentration $N_d = 10^{18}$ cm^{-3}), and a 100 nm n-$Al_{0.25}Ga_{0.75}As$ cladding layer ($N_d = 10^{18}$ cm^{-3}). Figure 1 shows the energy band profiles, E_c and E_v, and the quasi-Fermi level profiles, E_{Fc} and E_{Fv}, along the growth direction z of the conduction and the valence bands, respectively, for the structure under a forward bias of 1.4 V, resulting from a self-consistent calculation to be described. The band profiles are given by

$$E_c(z) = E_{c0}(z) - q\Phi(z),$$

$$E_v(z) = E_{v0}(z) - q\Phi(z), \tag{1}$$

where E_{c0} and E_{v0} are the flat band profiles of the conduction and the valence bands, respectively, and Φ is the electrostatic potential. In our model, the central problem is to find the potential Φ and the quasi-Fermi levels, E_{Fc} and E_{Fv}, by solving self-consistently three coupled differential equations, including the one-dimensional Poisson equation,

$$\frac{d}{dz}\epsilon\frac{d}{dz}\Phi = -q(p - n + N_d^+ - N_a^-), \tag{2}$$

and the one-dimensional continuity equations of electrons and holes in the steady state,

$$dJ_n/dz = qR,$$

$$dJ_p/dz = -qR, \tag{3}$$

where ϵ is the electric permittivity, n, p, N_d^+, and N_a^- are the densities of electrons, holes, ionized donors, and ionized acceptors, respectively, J_n (J_p) is the current density due to the electron (hole) flow, and R is the net electron-hole recombination rate. The aforementioned n, p, N_d^+, N_a^-, J_n, J_p, and R are all functions of position z. They can be expressed in terms of Φ, E_{Fc}, and E_{Fv}. For the first six ones, we use the following formulas:

$$n = N_c\mathcal{F}_{1/2}(\eta_n), \quad \eta_n \equiv (E_{Fc} - E_c)/k_BT, \tag{4}$$

$$p = N_v\mathcal{F}_{1/2}(\eta_p), \quad \eta_p \equiv (E_v - E_{Fv})/k_BT, \tag{5}$$

$$N_d^+ = N_d/[1 + 2e^{(E_{Fc}-E_d)/k_BT}], \tag{6}$$

$$N_a^- = N_a/[1 + 4e^{(E_a-E_{Fv})/k_BT}], \tag{7}$$

$$J_n = -qn\mu_n d\Phi/dz + qD_n dn/z, \tag{8}$$

$$J_p = -qp\mu_p d\Phi/dz - qD_p dp/dz, \tag{9}$$

where N_c (N_v) is the effective density of states of the conduction (valence) band, $\mathcal{F}_j$ is the Fermi–Dirac integral of order j,[21]

$$\mathcal{F}_j(\eta) = \frac{1}{\Gamma(j+1)}\int_0^\infty \frac{\xi^j d\xi}{e^{\xi-\eta}+1}, \tag{10}$$

E_d (E_a) is the donor (acceptor) level, μ_n (μ_p) is the electron (hole) mobility, and D_n (D_p) is the electron (hole) diffusion coefficient, which can be related to the mobility by[22]

$$D_i = \mu_i\frac{k_BT}{q}\frac{\mathcal{F}_{1/2}(\eta_i)}{\mathcal{F}_{-1/2}(\eta_i)}, \quad i = n,p. \tag{11}$$

For the recombination rate R, we consider the radiative, the Auger, and the Shockley–Read–Hall (SRH) recombinations in the high-quality GaAs active layer. On the other

[This article is copyrighted as indicated in the article. Reuse of AIP content is subject to the terms at: http://scitation.aip.org/termsconditions. Downloaded to] IP: 140.113.38.11 On: Wed, 30 Apr 2014 11:57:17

hand, in the other layers containing aluminum, the recombination process is assumed to be dominated by the SRH recombination for simplicity.[23] Therefore, we write

$$R = \begin{cases} R_{\text{rad}} + R_{\text{Aug}} + R_{\text{SRH}} & z \text{ in the active layer}, \\ R_{\text{SRH}} & \text{otherwise}, \end{cases} \tag{12}$$

where R_{rad}, R_{Aug}, and R_{SRH} are the radiative, the Auger, and the SRH recombination rates, respectively. In calculating R_{rad}, we neglect the stimulated emission and consider only the spontaneous emission involving the electric-dipole transitions from the conduction (C) to both the heavy-hole (HH) and the light-hole (LH) bands. As a result, R_{rad} is obtained from the integral

$$R_{\text{rad}} = \int r(\hbar\omega) d\hbar\omega, \quad r = r_{\text{hh}} + r_{\text{lh}}, \tag{13}$$

where $\hbar$ is the reduced Planck constant, ω is the optical angular frequency, r is the total spontaneous emission rate, and r_{hh} (r_{lh}) is the contribution of the $\text{C} \to \text{HH}(\text{C} \to \text{LH})$ transitions to r. For r_{hh}, we use the formula[24]

$$r_{\text{hh}}(\hbar\omega) = C_{\text{hh}} \frac{\hbar\omega\sqrt{\hbar\omega - E_g}\,\Theta(\hbar\omega - E_g)}{\left[1 + e^{-\eta_n} \exp\left(\dfrac{m_r}{m_c}\dfrac{\hbar\omega - E_g}{k_BT}\right)\right]\left[1 + e^{-\eta_p} \exp\left(\dfrac{m_r}{m_{\text{hh}}}\dfrac{\hbar\omega - E_g}{k_BT}\right)\right]}, \tag{14}$$

where

$$C_{\text{hh}} = \frac{q^2 n_r m_r^{3/2} E_P}{3\sqrt{2}\pi^3 \epsilon_0 m_0 \hbar^5 c^3}. \tag{15}$$

ϵ_0, m_0, and c are the permittivity, the electron mass, and the light speed, respectively, *in vacuo*, m_c and m_{hh} are the effective masses of electrons in the conduction and holes in the HH bands, respectively, m_r is the reduced mass $m_r = m_c m_{\text{hh}}/(m_c + m_{\text{hh}})$, n_r is the refractive index, E_P is the optical matrix parameter, and Θ is the unit step function. For r_{lh}, just replace the role of m_{hh} in Eq. (14) by the LH mass m_{lh}. In deduction of Eq. (14), the parabolic band approximation has been used. For calculating R_{Aug}, we consider the CHHS and CHCC processes and use the form[25]

$$R_{\text{Aug}} = (C_p p + C_n n)(pn - n_i^2), \tag{16}$$

where C_p (C_n) is the Auger coefficient for CHHS (CHCC) process and $n_i = \sqrt{N_c N_v} e^{-E_g/2k_BT}$ is the intrinsic carrier density. For R_{SRH}, we use the well-known formula[26]

$$R_{\text{SRH}} = \frac{pn - n_i^2}{\tau_n(p + n_i) + \tau_p(n + n_i)}, \tag{17}$$

where τ_n (τ_p) is the lifetime parameter that has a meaning of the minority carrier lifetime if $p \gg n, n_i (n \gg p, n_i)$.

The above drift-diffusion model is applicable only for the carrier transport within each layer but not for the transport across the heterojunction interfaces and at the two end surfaces. To determine unambiguously the set of Φ, E_{Fc}, and E_{Fv} for each applied voltage V, we have to further specify the boundary conditions at the interfaces and surfaces. The boundary condition for Φ is simply the continuities of Φ and $\epsilon d\Phi/dz$. However, those for E_{Fc} and E_{Fv} are more complicated. The carrier flow across an interface is governed by the thermionic emission process if the band offset at the interface is large. In this case, the notion of quasi-Fermi levels, which is used in the drift-diffusion model, is inappropriate around the interface. A more suitable model for the problem is the thermionic emission model which allows the quasi-Fermi levels to be discontinuous at the interface.[27] For the current along the positive z direction, as in the case of Fig. 1, the thermionic emission current density due to electron flow across an interface at z_i can be expressed as[27,28]

$$J_n(z_i) = A_n(z_i^+) T^2 \mathcal{F}_1[\xi_n(z_i^+)] - A_n(z_i^-) T^2 \mathcal{F}_1[\xi_n(z_i^-)], \tag{18}$$

where $z_i^{\pm} = \lim_{\varepsilon \to +0}(z_i \pm \varepsilon)$, A_n $(z_i^{\pm})$ is the effective Richardson constant of the electron at $z_i^{\pm}$, and ξ_n $(z_i^{\pm})$ is defined as

$$\xi_n(z_i^{\pm}) = \frac{E_{Fc}(z_i^{\pm}) - \max[E_c(z_i^+), E_c(z_i^-)]}{k_BT}. \tag{19}$$

Similarly, the thermionic emission current density due to hole flow across the interface at z_i is

$$J_p(z_i) = A_p(z_i^-) T^2 \mathcal{F}_1[\xi_p(z_i^-)] - A_p(z_i^+) T^2 \mathcal{F}_1[\xi_p(z_i^+)], \tag{20}$$

where A_p $(z_i^{\pm})$ is the effective Richardson constant of the hole at $z_i^{\pm}$ and ξ_p $(z_i^{\pm})$ is defined as

$$\xi_p(z_i^{\pm}) = \frac{\min[E_v(z_i^+), E_v(z_i^-)] - E_{Fv}(z_i^{\pm})}{k_BT}. \tag{21}$$

Since the thermionic emission process is predominant only when the band offset is sufficiently large, we assume the quasi-Fermi level is continuous if the corresponding band offset is less than $2k_BT$. For the conduction band offset $|E_c(z_i^+) - E_c(z_i^-)| > 2k_BT$, the relation between E_{Fc} (z_i^+) and E_{Fc} (z_i^-) is determined by the continuity of J_n at z_i, i.e.,[27]

$$J_n(z_i) = J_n(z_i^{\pm}), \tag{22}$$

where J_n (z_i) is the thermionic emission current density of electrons given by Eq. (18) but J_n $(z_i^{\pm})$ is the drift-diffusion current density of electrons at $z_i^{\pm}$ [see Eq. (8)]. The boundary condition for E_{Fv} is determined by the continuity of J_p at the interface, similar to that for E_{Fc} just described above.

At the end surfaces on which the electrode contacts are supposed to be made, the surface recombination velocities are assumed to be infinite so that the carrier densities reach

[This article is copyrighted as indicated in the article. Reuse of AIP content is subject to the terms at: http://scitation.aip.org/termsconditions. Downloaded to] IP: 140.113.38.11 On: Wed, 30 Apr 2014 11:57:17

the values of thermal equilibrium and the Fermi levels are pinned at fixed positions from the band edges. The Fermi level positions at the surfaces are simply determined by the electric neutrality condition $p+N_d^+=n+N_a^-$, using Eqs. (4)–(7) with $E_{Fc}=E_{Fv}$.

With the boundary conditions at the interfaces and surfaces, the differential Eqs. (2) and (3) can be solved steadily by the numerical iteration method for each applied voltage V. The external electrical work qV done on each of the electrons from the cathode to the anode gives the Fermi level difference between the two surfaces $E_{Fc}|_{z \text{ at cathode}}-E_{Fv}|_{z \text{ at anode}}=qV$.

B. Quantities of interest

Once the solutions have been found, we can calculate the quantities of interest. For instance, the current density J, which has been determined for a given V, can be divided into various components which will be useful for later analysis,

$$J = J_{\text{inj}} + J_{\text{leak}}, \tag{23}$$

where J_{inj} is the injection current density attributed to the recombinations in the active layer and J_{leak} is the leakage current density due to recombinations outside the active layer. The injection current density can be further expressed as

$$J_{\text{inj}} = J_{\text{rad}} + J_{\text{Aug}} + J_{\text{SRH(act)}}, \tag{24}$$

where J_{rad}, J_{Aug}, and $J_{\text{SRH(act)}}$ are the components due to the radiative, the Auger, and the SRH recombinations, respectively, in the active region

$$J_i = q\int_{\text{active layer}} R_i dz, \quad i = \text{rad, Aug, SRH}. \tag{25}$$

We can obtain J_{leak} by simply employing $J_{\text{leak}}=J-J_{\text{inj}}$ or by considering it as composed of the electron and the hole leakage current densities

$$J_{\text{leak}} = J_n(z_p) + J_p(z_n), \tag{26}$$

where z_p (z_n) is at the interface between the active and the spacer layers near the p (n) region. Obviously, J_n (z_p) [$J_p(z_n)$] is the current density due to electron (hole) flow across the interface z_p (z_n) from the active region. Since the recombinations out of the active layer include the SRH recombination and the surface recombination at electrodes, J_{leak} can also be written as

$$J_{\text{leak}} = J_{\text{SRH(leak)}} + J_{\text{sr}}, \tag{27}$$

where $J_{\text{SRH(leak)}}$ is due to the SRH recombination outside the active layer

$$J_{\text{SRH(leak)}} = q\int_{z \notin \text{active layer}} R_{\text{SRH}} dz, \tag{28}$$

and J_{sr} is due to the surface recombination

$$J_{\text{sr}} = J_n|_{z \text{ at anode}} + J_p|_{z \text{ at cathode}}. \tag{29}$$

The terms of the injection efficiency η_{inj} and the internal efficiency η_{int} will be used for later analysis. They are defined as

$$\eta_{\text{inj}} = J_{\text{inj}}/J, \tag{30}$$

$$\eta_{\text{int}} = J_{\text{rad}}/J_{\text{inj}}. \tag{31}$$

The ideal radiative power density is calculated by

$$P_{\text{rad}}^0 = \int\int r\hbar\omega d\hbar\omega dz = \langle\hbar\omega\rangle J_{\text{rad}}/q. \tag{32}$$

It is the power density of all the photons generated in the active region, no matter whether or not they can escape out of the device. The realistic radiative power density P_{rad} out of the device depends on the photon escape capability and the photon recycling effect.[29,30] In fact, the photon recycling and escape depend on the geometry, the parasitic loss, and the surface texture of the device.[30] A detailed consideration of these effects should be another subject and is out of the scope of the present work. In this work, we define the extraction efficiency of radiative power η_{xp} to be the proportionality constant between P_{rad} and P_{rad}^0

$$P_{\text{rad}} = \eta_{\text{xp}} P_{\text{rad}}^0. \tag{33}$$

It will be used as a parameter to account for the photon escape efficiency. For simplicity, we do not consider the photon recycling in the calculation, i.e., we assume that the energy of photons that are captured in the device would totally become heat through parasitic absorption.

The electric input power density is JV. It has been assumed explicitly that the device is kept at a steady temperature T even under a bias V. This means that there is heat flowing into or out of the device to keep the temperature steady. The cooling power density P_c, defined to be the power density of the heat required to flow into the device, is therefore

$$P_c = P_{\text{rad}} - JV. \tag{34}$$

It is convenient for analysis to define the ideal cooling power density $P_c^0=P_{\text{rad}}^0-JV$, which is P_c with η_{xp} set at unity. Then, P_c can be written explicitly in terms of the parameter η_{xp}

$$P_c = \eta_{\text{xp}}(P_c^0 + JV) - JV. \tag{35}$$

From Eq. (34), the criterion for cooling action ($P_c>0$) can be written as

$$\eta_{\text{ext}} > qV/\langle\hbar\omega\rangle \equiv \eta_{\text{ext,cr}} \tag{36}$$

or

$$\eta_{\text{xp}} > \eta_{\text{ext,cr}}/(\eta_{\text{inj}}\eta_{\text{int}}) \equiv \eta_{\text{xp,cr}}, \tag{37}$$

where $\eta_{\text{ext}}=\eta_{\text{xp}}\eta_{\text{inj}}\eta_{\text{int}}$ is called the external efficiency or the overall efficiency. In deriving the criterion, we have used Eqs. (30), (31), and (33).

For conventional TE coolers, the coefficient of performance (COP) is used as a measure of cooling efficiency. It is defined as the ratio of the heat removed from the cold side (or the heat load) to the input work. The EL (or PL) coolers work as a heat sink, absorbing heat energy from the heat load and transferring it into optical energy. At steady state, the

[This article is copyrighted as indicated in the article. Reuse of AIP content is subject to the terms at: http://scitation.aip.org/termsconditions. Downloaded to] IP: 140.113.38.11 On: Wed, 30 Apr 2014 11:57:17

TABLE I. Some of the parameters of $Al_xGa_{1-x}As$ used in the calculation.

Parameters	$Al_xGa_{1-x}As$
E_g (eV)	$1.424+1.247x$
ϵ/ϵ_0	$12.9-2.84x$
m_c/m_0	$0.063+0.083x$
m_{hh}/m_0	$0.51+0.25x$
m_{lh}/m_0	$0.082+0.068x$

cooling power is equal to the rate at which the heat is removed from the load. It is therefore proper to define the cooling efficiency η_c (or COP) for the EL coolers to be the ratio of the cooling power to the input power

$$\eta_c = \frac{P_c}{JV} = \frac{\eta_{ext}}{\eta_{ext,cr}} - 1. \tag{38}$$

In terms of η_{xp} explicitly,

$$\eta_c = \eta_{xp}(\eta_c^0 + 1) - 1, \tag{39}$$

where η_c^0 is the cooling efficiency with η_{xp} set at unity. Using Eq. (35) or (39), the critical extraction efficiency $\eta_{xp,cr}$ can also be expressed as

$$\eta_{xp,cr} = \frac{1}{1 + \eta_c^0}. \tag{40}$$

Equations (35), (38), and (40) allow us to express P_c as

$$P_c = P_c^0\left(1 - \frac{1 - \eta_{xp}}{1 - \eta_{xp,cr}}\right). \tag{41}$$

C. Parameters used for the calculation

In our calculation, the temperature is set at 300 K. Some of the parameters of $Al_xGa_{1-x}As$ used are listed in Table I. The conduction band offset ΔE_c is set to be 60% of the band offset ΔE_g. The effective densities of states are given by $N_c = 2.5\times 10^{19}(m_c/m_0)^{3/2}$ cm^{-3} and $N_v = 2.5\times 10^{19}[(m_{hh}/m_0)^{3/2} + (m_{lh}/m_0)^{3/2}]$ cm^{-3}.[31] The mobilities μ_n and μ_p are obtained from the empirical model in Ref. 32. The effective Richardson constants are given by $A_n = Am_c/m_0$ and $A_p = A(m_{hh}+m_{lh})/m_0$, where $A = 120$ A/cm^2 K^2 is the Richardson constant.[31] We take the refractive index $n_r = 3.6$, the optical matrix parameter $E_P = 25.7$ eV, the lifetime parameters $\tau_n = 1.3\times 10^{-6}$ s and $\tau_p = 1.2\times 10^{-6}$ s for the SRH recombination, and the Auger coefficients[33] $C_n = 1.0\times 10^{-31}$ cm^6/s and $C_p = 1.2\times 10^{-30}$ cm^6/s for GaAs. The binding energies of the donors and the acceptors ($E_c - E_d$ and $E_a - E_v$) are assumed to be k_BT for simplicity. In the layers containing aluminum, the lifetime parameters τ_n and τ_p for the SRH recombination are set at 10^{-8} s. It is not required to use accurate values for the binding energies and the lifetime parameters in these cladding layers. They will not influence significantly our calculated results because of the short cladding layers of high conductivity.

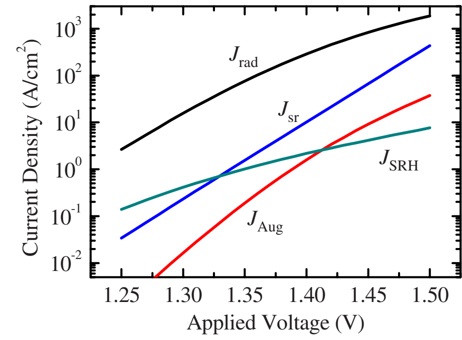

FIG. 2. (Color online) The current density components J_{rad}, J_{Aug}, J_{SRH}, and J_{sr} vs the applied voltage V for the heterostructure with an active layer of width $L=0.1$ μm and carrier blocking layers of Al composition $x=0.25$, which have no effect on blocking carriers.

III. RESULTS AND DISCUSSION

In this section we present and analyze the results on the EL cooling in the heterostructure under consideration, calculated by the self-consistent model described in the Sec. II.

Figure 2 shows the current density components, including J_{rad}, J_{Aug}, J_{SRH}, and J_{sr}, versus the applied voltage V for the heterostructure containing an active layer of width $L = 0.1$ μm and carrier blocking layers of Al composition $x = 0.25$. Here, $J_{SRH} = J_{SRH(act)} + J_{SRH(leak)}$. Since the cladding and the spacer layers also have an Al composition of 0.25, the carrier blocking layers here have no effect on blocking carriers. As the figure shows, while the radiative recombination current density J_{rad} is the major component, the nonradiative current density ($J_{sr}+J_{SRH}+J_{Aug}$) plays a nonnegligible part, especially at a high voltage, even though it is less than 10% of the total current density. As will be shown later, a small amount of current loss can cause the device to fail in cooling when V is close to the value E_g/q, at which the critical external efficiency $\eta_{ext,cr}$ may be close to or larger than unity. The dissipation is contributed mostly by the surface recombination due to the narrow cladding layers. Increasing the thickness of the cladding layers can reduce the surface recombination[19] but enhance the SRH recombination. Furthermore, it requires a cladding layer thickness of more than the carrier diffusion length (~ 10 μm) to alleviate effectively the surface recombination, leading to a long time for epitaxy.

An alternative way to simultaneously reduce the leakage current effectively and keep short cladding layers is to employ the carrier blocking layers. We show in Fig. 3(a) the effect of the blocking layers by plotting the curves of the injection efficiency η_{inj} versus V for different Al compositions of the blocking layers, $x = 0.25$, 0.3, 0.35, and 0.4. It is evident that η_{inj} can be improved significantly by increasing the barrier height of the blocking layers when $x \leq 0.3$. The improvement becomes insignificant as x increases from 0.35 to 0.4 because the leakage current across the blocking layers has almost been eliminated when $x = 0.35$. In this case, the residue of leakage current is mostly due to the SRH recombination in the spacer layers. As a result, η_{inj} increases and approaches 100% with V for $x \geq 0.35$. Differently, for $x \leq 0.3$, η_{inj} first increases slightly and then decreases rapidly

[This article is copyrighted as indicated in the article. Reuse of AIP content is subject to the terms at: http://scitation.aip.org/termsconditions. Downloaded to] IP: 140.113.38.11 On: Wed, 30 Apr 2014 11:57:17

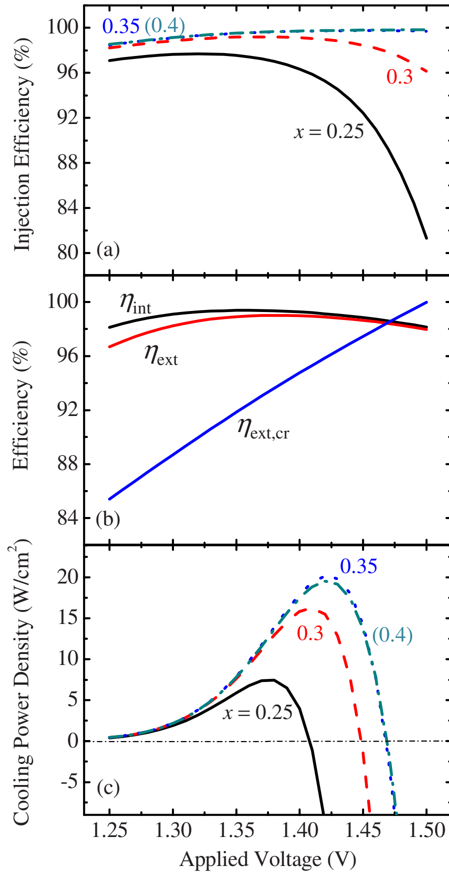

FIG. 3. (Color online) (a) The injection efficiency η_{inj}, (b) the efficiencies η_{int}, η_{ext}, and $\eta_{ext,cr}$ (with $\eta_{xp}=1$), and (c) the ideal cooling power density P_c^0 (with $\eta_{xp}=1$) vs V. In (a) and (c), the curves are plotted for different barrier heights of the blocking layers $x=0.25$, 0.3, 0.35, and 0.4. In (b) the curves are for $x=0.4$.

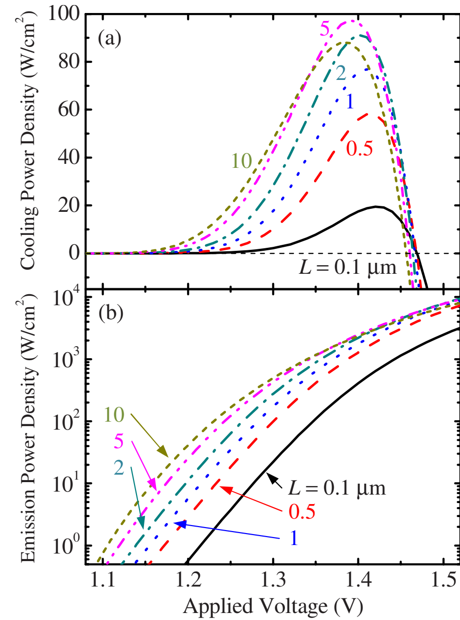

FIG. 4. (Color online) (a) The ideal cooling power density P_c^0 and (b) the ideal radiative power density P_{rad}^0 as functions of V for structures with the same blocking layers ($x=0.4$) but different active layer thicknesses $L=0.1$, 0.5, 1, 2, 5, and 10 μm.

with V because of the rapid increase in leakage current. In contrast to η_{inj}, the internal efficiency η_{int} and the average photon energy $\langle \hbar\omega \rangle$ (and hence the critical external efficiency $\eta_{ext,cr}$) are practically independent of x. Figure 3(b) shows η_{int}, η_{ext}, and $\eta_{ext,cr}$ versus V for $x=0.4$ and $\eta_{xp}=1$. The internal efficiency η_{int} has a maximum at $V=1.35$ V and declines at lower and higher V because $J_{SRH(act)}$ (J_{Aug}) plays a more important part at a lower (higher) V. The $\eta_{ext,cr}$ increases almost linearly with V because $\langle \hbar\omega \rangle$ is almost independent of V [referring to Eq. (36)]. For the cooling power density P_c to be positive, V has to be less than the critical voltage V_{cr} at which η_{ext} crosses with $\eta_{ext,cr}$. Here, $V_{cr}=1.47$ V for $x=0.4$. Obviously, V_{cr} is smaller for a smaller x because of lower η_{ext}. This can be seen in Fig. 3(c), which shows the ideal cooling power density P_c^0 (with $\eta_{xp}=1$) versus V for different barrier heights of the blocking layers ($x=0.25$, 0.3, 0.35, and 0.4). It is also found that increasing x can increase not only V_{cr} but also the maximum of the ideal cooling power density $P_{c,max}^0$, which is increased from 7.5 to 20 W/cm^2 as x increases from 0.25 to 0.35. Further increasing x beyond 0.35 hardly changes P_c^0, consistent with the variation in η_{inj} in Fig. 3(a). With the blocking layers, we can avoid using cladding layers of high Al content which is not preferred for optoelectronic devices due to the reliability issue.

The cooling power density of 20 W/cm^2 seems to be the limiting value for the structure with the active layer thickness of $L=0.1$ μm. To further enhance it, one can increase the active layer thickness. Intuitively, a wider active layer can contain more electron-hole pairs at a given V, corresponding to a higher total radiative recombination rate J_{rad}/q. Figure 4 shows the ideal cooling power density P_c^0 in Fig. 4(a) and the ideal radiative power density P_{rad}^0 in Fig. 4(b) as functions of V for the structures with the same blocking layers ($x=0.4$) but different active layer thicknesses $L=0.1$, 0.5, 1, 2, 5, and 10 μm. The maximum cooling power density $P_{c,max}^0$ can be improved about five times up to as high as 97 W/cm^2 by increasing L from 0.1 to 5 μm. The improvement is prominent only when $L \leq 5$ μm. For $L > 5$ μm, increasing L does not improve but degrades $P_{c,max}^0$ due to the remarked nonuniformity of carrier distributions, as L is comparable to or greater than the carrier diffusion lengths. From our calculation, we find that the average carrier density in the active layer is lower for a larger L; this difference in the average carrier density between different L's is particularly remarkable when V is high. This explains the fact that P_c^0 for $L=10$ μm is higher (lower) than for $L=5$ μm at a low (high) V. The radiative power density can also be improved greatly by increasing L. This is important if the device is used for the purpose of light emitting.

The result of Fig. 4(a) suggests the device to be with a 5 μm active layer and biased at about 1.39 V for a maximum cooling power. However, the result is obtained under the unrealistic assumption $\eta_{xp}=1$. In practice, such a high extraction efficiency is almost unattainable especially when L is larger than 1–2 μm, the inverse of the absorption coefficient of the active layer. A slight deviation of η_{xp} from unity may cause P_c to become negative if V is high, such that $JV \gg P_c^0$ (or $\eta_{xp,cr} \approx 1$), as can be understood from Eq. (35)

[This article is copyrighted as indicated in the article. Reuse of AIP content is subject to the terms at: http://scitation.aip.org/termsconditions. Downloaded to] IP: 140.113.38.11 On: Wed, 30 Apr 2014 11:57:17

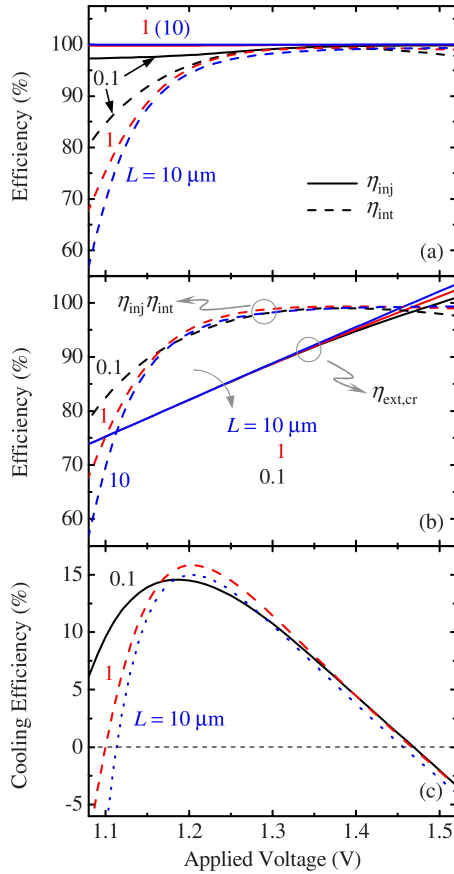

FIG. 5. (Color online) (a) The injection efficiency η_{inj} and the internal efficiency η_{int}, (b) the product $\eta_{inj}\eta_{int}$ and the critical external efficiency $\eta_{ext,cr}$, and (c) the cooling efficiency η_c^0 (with η_{xp}=1) vs V for structures with different active layer thicknesses L=0.1, 1, and 10 μm. The Al content of the blocking layers is set at x=0.4.

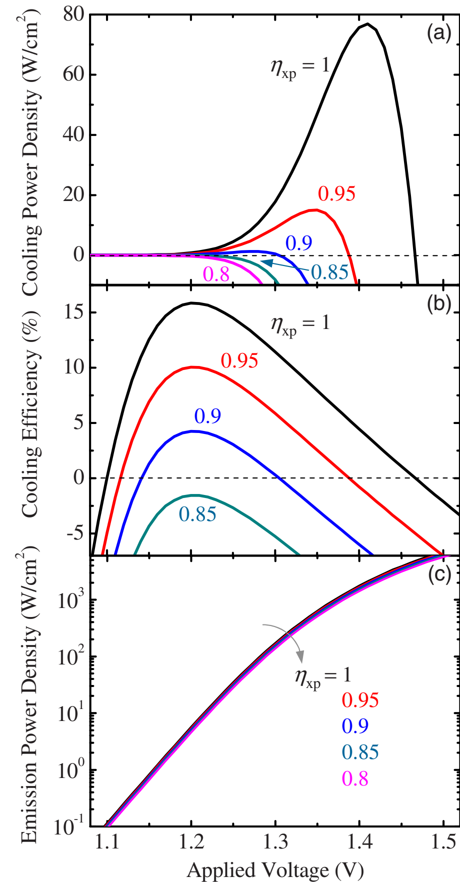

FIG. 6. (Color online) (a) The cooling power density P_c, (b) the cooling efficiency η_c, and (c) the radiative power density P_{rad} as functions of V for the structure with a 1 μm active layer and $Al_{0.4}Ga_{0.6}As$ blocking layers, with different extraction efficiencies η_{xp}=0.8, 0.85, 0.9, 0.95, and 1.

[or Eq. (41)]. On the other hand, $J_{SRH(act)}$ becomes important when the device is biased at a low V. There arises the issue of design margin.

Figure 5 shows the injection efficiency η_{inj} and the internal efficiency η_{int} in Fig. 5(a), the product $\eta_{inj}\eta_{int}$ and the critical external efficiency $\eta_{ext,cr}$ in Fig. 5(b), and the cooling efficiency η_c^0 (with η_{xp}=1) in Fig. 5(c) versus V for the structures with different active layer thicknesses L=0.1, 1, and 10 μm. Here, the Al content of the blocking layers is set at x=0.4 Since J_{inj} is enhanced by increasing L, η_{inj} is also enhanced. For $L \gtrsim 1$ μm, η_{inj} is nearly 100%, almost independent of V. As has been described for Fig. 3(b), η_{int} has a maximum at about V=1.37 V. It then declines more profoundly as V decreases than increases, implying that the SRH recombination is more important at lower V than the Auger recombination at higher V. Such lowering of η_{int} at low V is more prominent for larger L because of a lower carrier density in the wider active region. The lower carrier density for a larger L can be understood by noting that the current and the voltage drop outside the active region are larger for a larger L. This causes a smaller $E_{Fc}-E_{Fv}$ and thus the lower carrier density in the active region. On the other side, at high V, the Auger recombination is less important for a larger L due also to the lower carrier density, leading to a higher η_{int}. The ratio $\eta_{ext,cr}/(\eta_{inj}\eta_{int})$, which is $\eta_{xp,cr}$ [see Eq. (37)], gives the design margin for η_{xp}. For instance, at V=1.2 V and for L=10 μm, $\eta_{inj}\eta_{int}$=94% and $\eta_{ext,cr}$=82%, as can be found from Fig. 5(b), give $\eta_{xp,cr}$=87%. This implies that η_{xp} has to be greater than 87% for the device to act in the cooling mode; otherwise, the device will generate heat. Evidently, the margin becomes tighter when V either increases or decreases from 1.2 V. If V is too high or too low, $\eta_{xp,cr}>1$ and the cooling coefficient η_c^0 is negative [Fig. 5(c)]. In this case, it is impossible for the device to act in the cooling mode. At V=1.39 V at which the maximum cooling power occurs [as shown in Fig. 4(a)], $\eta_{xp,cr}$=96% for L=10 μm. Such a high efficiency is difficult to achieve by the state-of-the-art technology for EL devices. The value of $\eta_{xp,cr}$ can also be derived from the curves for η_c^0 in Fig. 5(c) through Eq. (40). The η_c^0 decreases from its maximum as V departs from the voltage about 1.2 V. It can be as high as 15% at about V =1.2 V but only about 4% at V=1.39 V.

Figure 6(a)–6(c) show the cooling power density P_c, the cooling efficiency η_c, and the radiative power density P_{rad}, respectively, as functions of V for the structure of a 1 μm active layer and $Al_{0.4}Ga_{0.6}As$ blocking layers, with different extraction efficiencies, η_{xp}=0.8, 0.85, 0.9, 0.95, and 1. As can be seen in Fig. 6(a), a slight reduction in η_{xp} from 100% to 95% leads to a dramatic change in P_c at a high V. The high P_c of 79 W/cm^2 at 1.41 V reduces to a negative value when η_{xp} is changed from 100% to 95%. This indicates the

[This article is copyrighted as indicated in the article. Reuse of AIP content is subject to the terms at: http://scitation.aip.org/termsconditions. Downloaded to] IP: 140.113.38.11 On: Wed, 30 Apr 2014 11:57:17

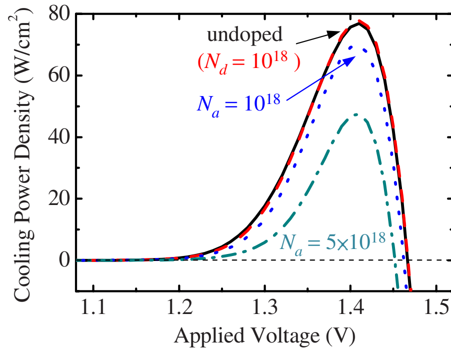

FIG. 7. (Color online) The ideal cooling power density P_c^0 as a function of V for the active regions which are undoped, doped with $N_d=10^{18}$ cm^{-3}, with $N_a=10^{18}$ cm^{-3}, and with $N_a=5\times10^{18}$ cm^{-3}. The active layer thickness is $L=1$ μm and the Al content of the blocking layers is $x=0.4$.

susceptibility of the device to the efficiency as it is biased at a high voltage. The situation becomes gentler at a lower electric bias. At $V=1.3$ V, P_{rad} can be as high as about 150 W/cm^2 for $\eta_{\text{xp}}\geq 90\%$ and, simultaneously, P_c can be nonnegative. At $V=1.2$ V, where the maximum η_c occurs for each η_{xp}, the $\eta_c=0$ and $P_{\text{rad}}\approx 40$ W/cm^2 for $\eta_{\text{xp}}=87\%$.

Although the results show that the EQE required for EL cooling ($\eta_{\text{ext}}\approx 87\%$) can be significantly lower than for PL cooling ($\eta_{\text{ext}}\approx 97\%$), the high η_{xp} of 87% is still difficult to achieve. It is noticed that we have neglected the photon recycling in the calculation, i.e., we have assumed that all the photon trapped in the device were absorbed to generate heat. In fact, when the photon recycling is considered, it is probably the case that most of the trapped photons are reabsorbed to generate new electron-hole pairs. Only a small amount of the trapped radiative energy is transferred into heat by parasitic absorption. In other words, what determines the device to act in the cooling mode or not essentially is the optical parasitic loss of the material if the device is properly biased. With the photon recycling taken into correction, the EQE and the critical extraction efficiency are[34]

$$\eta_{\text{ext}} = \frac{\eta_{\text{inj}}\eta_{\text{int}}\eta_{\text{xp}}}{1-\eta_{\text{int}}\eta_{\text{pr}}(1-\eta_{\text{xp}})}, \tag{42}$$

$$\eta_{\text{xp,cr}} = \frac{1-\eta_{\text{inj}}\eta_{\text{pr}}}{\eta_{\text{int}}(\eta_{\text{inj}}\langle\hbar\omega\rangle/qV-\eta_{\text{pr}})} > 0, \tag{43}$$

where η_{pr} is the photon recycling efficiency defined as the fraction of trapped photons which are reabsorbed to generate new electron-hole pairs. If the parasitic loss is low (1% or $\eta_{\text{pr}}=0.99$, for instance), only a small value (10% or less) of η_{xp} can result in a high EQE ($\eta_{\text{ext}}>90\%$ which can safely be larger than $\eta_{\text{ext,cr}}=qV/\langle\hbar\omega\rangle$) and net cooling.[6]

Figure 7 shows the ideal cooling power density P_c^0 as a function of V for the active regions which are undoped, doped with $N_d=10^{18}$ cm^{-3}, with $N_a=10^{18}$ cm^{-3}, and with $N_a=5\times10^{18}$ cm^{-3}. Here, the thickness of all the active layer is $L=1$ μm and the Al content of the blocking layers is $x=0.4$. We find that intentionally doping into the active region does not improve the cooling power. Furthermore, the calculated cooling power density may be overestimated for the doped active regions because we do not consider exactly the dopant-assisted SRH and Auger processes.[33] The degradation caused by the p-type doping is mainly due to the enhanced Auger recombination. The n-type doping, suppressing both the radiative and the Auger recombinations, leads to a slight reduction in P_c^0 at low V.

What is also important in the present work is that we put bounds to the cooling power density and the applied voltage for EL cooling, no matter whether the photon recycling is taken into account. For the same device structures, the curves for $\eta_{\text{xp}}=1$ in Figs. 4, 5(c), 6, and 7 provide the upper bounds to those for $\eta_{\text{xp}}<1$ even if the photon recycling is considered. This is because the η_{ext} in Eq. (42) has a maximum $\eta_{\text{inj}}\eta_{\text{int}}$, which is just the η_{ext} when $\eta_{\text{xp}}=1$. As a result, Fig. 4(a) gives the limiting cooling power density of 97 W/cm^2; devices with a GaAs active region must give a cooling power density not more than the limiting value at 300 K, even if the photon recycling efficiency is 100%. Figure 5(c) provides the information on the upper and lower bounds to the applied voltage for net EL cooling. For instance, the device with $L=1$ μm should be biased between 1.1 and 1.46 V for net cooling. The voltage range for net cooling in the realistic case ($\eta_{\text{xp}}<1$) must lie between the bounds.

IV. CONCLUSION

We have presented an analysis of the results calculated by a self-consistent model for electroluminescent refrigeration and also for light emitting without heat generation in heterostructures. It has been found that the cooling related quantities, such as the maximum cooling power density, the cooling efficiency, and the critical voltage below which the device acts in the cooling mode, are sensitive to the overall efficiency due to the small ratio of the thermal energy to the band gap. The injection efficiency can be improved to nearly 100% by employing carrier blocking layers of $Al_xGa_{1-x}As$ ($x\geq 0.35$) near the GaAs active layer. A GaAs active layer with thickness of about 5 μm at 300 K can give an internal efficiency of nearly 100% and a limiting cooling power density of 97 W/cm^2. A smaller thickness of the active layer gives a higher Auger recombination rate at a high voltage, while a larger one may cause a nonuniform distribution of carriers, reducing the radiative power. For an EL device to work without generating heat, it requires an external efficiency of 87%, which is lower than for a PL device by 10%, revealing the advantage of an EL device in luminescent cooling. For a cooling power density more than several W/cm^2, the external efficiency has to be more than 90%. For the light-emitting purpose, it is likely to realize a high output power of more than 100 W/cm^2 without heating by making the external efficiency higher than 90%. The high external efficiency can easily be achieved if the photon recycling efficiency is high.

ACKNOWLEDGMENTS

This work was supported by National Science Council of the Republic of China under Contract No. 97-2221-E-009-164.

[This article is copyrighted as indicated in the article. Reuse of AIP content is subject to the terms at: http://scitation.aip.org/termsconditions. Downloaded to] IP: 140.113.38.11 On: Wed, 30 Apr 2014 11:57:17

[1]For an overview of optical refrigeration in solids, see M. Sheik-Bahae and R. I. Epstein, Laser Photonics Rev. **3**, 67 (2009); Nat. Photonics **1**, 693 (2007).
[2]R. I. Epstein, M. I. Buchwald, B. C. Edwards, T. R. Gosnell, and C. E. Mungan, Nature (London) **377**, 500 (1995).
[3]R. Frey, F. Micheron, and J. P. Pocholle, J. Appl. Phys. **87**, 4489 (2000).
[4]G. Mills and A. Mord, Cryogenics **46**, 176 (2006).
[5]M. Sheik-Bahae and R. I. Epstein, Phys. Rev. Lett. **92**, 247403 (2004).
[6]J.-B. Wang, S. R. Johnson, D. Ding, S.-Q. Yu, and Y.-H. Zhang, J. Appl. Phys. **100**, 043502 (2006).
[7]G. Rupper, N. H. Kwong, and R. Binder, Phys. Rev. B **76**, 245203 (2007).
[8]H. Gauck, T. H. Gfroerer, M. J. Renn, E. A. Cornell, and K. A. Bertness, Appl. Phys. A: Mater. Sci. Process. **64**, 143 (1997).
[9]T. H. Gfroerer, E. A. Cornell, and M. H. Wanlass, J. Appl. Phys. **84**, 5360 (1998).
[10]B. Imangholi, M. P. Hasselbeck, M. Sheik-Bahae, R. I. Epstein, and S. Kurtz, Appl. Phys. Lett. **86**, 081104 (2005).
[11]S. Eshlaghi, W. Worthoff, A. D. Wieck, and D. Suter, Phys. Rev. B **77**, 245317 (2008).
[12]R. J. Keyes and T. M. Quist, Proc. IRE **50**, 1822 (1962).
[13]G. C. Dousmanis, C. W. Mueller, H. Nelson, and K. G. Petzinger, Phys. Rev. **133**, A316 (1964).
[14]P. Berdahl, J. Appl. Phys. **58**, 1369 (1985).
[15]A. G. Mal'shukov and K. A. Chao, Phys. Rev. Lett. **86**, 5570 (2001).
[16]S. Q. Yu, J. B. Wang, D. Ding, S. R. Johnson, D. Vasileska, and Y. H. Zhang, Solid-State Electron. **51**, 1387 (2007).
[17]P. Han, K. J. Jin, Y. L. Zhou, X. Wang, Z. S. Ma, S. F. Ren, A. G. Mal'shukov, and K. A. Chao, J. Appl. Phys. **99**, 074504 (2006).
[18]P. Han, K. J. Jin, Y. L. Zhou, H. B. Lu, and G. Z. Yang, J. Appl. Phys. **101**, 014506 (2007).
[19]O. Heikkilä, J. Oksanen, and J. Tulkki, J. Appl. Phys. **105**, 093119 (2009).
[20]Although there has been a self-consistent calculation performed for investigating the EL cooling in Refs. 17 and 18, unreasonable results, such as net cooling occurring at $V=1.6$ V which is obviously larger than $\langle \hbar\omega \rangle / q$ for GaAs, make the calculation unreliable.
[21]J. S. Blakemore, *Semiconductor Statistics* (Pergamon, New York, 1962).
[22]C. M. Wolfe, N. Holonyak, Jr., and G. E. Stillman, *Physical Properties of Semiconductors* (Prentice-Hall, New Jersey, 1989).
[23]R. K. Ahrenkiel, in *Gallium Arsenide and Related Compounds 1993: Proceedings of the 20th International Symposium on Gallium Arsenide and Related Compounds*, Freiburg, Germany, 29 August–2 September 1993, edited by H. S. Rupprecht and G. Weimann (Institute of Physics, London, 1994), pp. 685–690.
[24]S. L. Chuang, *Physics of Optoelectronic Devices* (Wiley, New York, 1995).
[25]V. N. Abakumov, V. I. Perel, and I. N. Yassievich, *Nonradiative Recombination in Semiconductors* (North-Holland, Amsterdam, 1991).
[26]W. Shockley and W. T. Read, Phys. Rev. **87**, 835 (1952).
[27]K. Horio and H. Yanai, IEEE Trans. Electron Devices **37**, 1093 (1990).
[28]M. D. Ulrich, P. A. Barnes, and C. B. Vining, J. Appl. Phys. **90**, 1625 (2001).
[29]I. Schnitzer, E. Yablonovitch, C. Caneau, and T. J. Gmitter, Appl. Phys. Lett. **62**, 131 (1993).
[30]R. Windisch, C. Rooman, S. Meinlschmidt, P. Kiesel, D. Zipperer, G. H. Döhler, B. Dutta, M. Kuijk, G. Borghs, and P. Heremans, Appl. Phys. Lett. **79**, 2315 (2001).
[31]S. M. Sze, *Physics of Semiconductor Devices* (Wiley, New York, 1981).
[32]M. Sotoodeh, A. H. Khalid, and A. A. Rezazadeh, J. Appl. Phys. **87**, 2890 (2000).
[33]M. Takeshima, Jpn. J. Appl. Phys., Part 1 **22**, 491 (1983).
[34]K.-C. Lee and S.-T. Yen (unpublished).

[This article is copyrighted as indicated in the article. Reuse of AIP content is subject to the terms at: http://scitation.aip.org/termsconditions. Downloaded to] IP: 140.113.38.11 On: Wed, 30 Apr 2014 11:57:17